Journal of Siberian Federal University. Mathematics & Physics 2013, 6(1), 3–17

УДК 532.68:536.25

On Thermocapillary Instability of a Liquid Column with a Co-axial Gas Flow

Victor K. Andreev*
Ilya I. Ryzhkov†
Institute of Computational Modelling, SB RAS,
Akademgorodok, 50/44, Krasnoyarsk, 660036 Russia

Received 09.07.2012, received in revised form 09.09.2012, accepted 01.10.2012

The thermocapillary flows and their stability in an infinite liquid column surrounded by a co–axial gas layer with a given flow rate are investigated. The gas layer is surrounded by a rigid cylindrical surface, which can move in vertical direction. A constant axial temperature gradient is maintained in the layers. The exact solution describing the stationary flow in the given two–phase system is derived. Possible flow regimes are investigated and linear stability analysis of these regimes is performed. The cases of non–deformable and deformable interface are studied.

Keywords: thermocapillary instability, two–phase system, liquid column.

Introduction

The study of two–phase systems with liquid–gas interfaces remains a challenging problem in fluid dynamics. In such systems, the variation of surface tension due to thermal gradient along the interface can cause convective flows in the bulk fluid [1]. Interfacial flows play an important role in many natural and technological processes, such as propagation of liquid jets, motion of thin liquid films, evolution of ocean waves, etc. A wide range of important applications promoted the development of different techniques for interfacial flow control.

Thermocapillary effect essentially affects the process of crystal growth by floating zone method [2]. To study the heat and fluid flow in the melt zone, a *liquid bridge model* is often used. In this model, the liquid is placed between two cylindrical rods (hot and cold) with a common axis. The surface tension gradient due to temperature variation along the free surface drives thermocapillary flow from hot to cold rod near the free surface and in the opposite direction at the axis. This flow is stationary for small temperature differences between the rods. The increase of temperature difference leads to the appearance of instability in the form of standing or travelling hydrothermal waves. This type of instability in the melt zone significantly reduces the crystal quality in the floating zone method [3].

Linear stability analysis of steady thermocapillary flow in an infinite liquid bridge was first performed by Xu and Davis [4]. These results were revisited by Ryzhkov [5]. It was shown that for large Prandtl number fluids the flow becomes unstable at much smaller values of the Marangoni number than it was reported previously. Experimental studies of instabilities in a long liquid bridge in microgravity were performed by Schwabe [6]. The obtained results are in good agreement with theoretical predictions [5]. The recent studies by Irikura *et al* [7] have shown that the heat exchange between liquid bridge and ambient gas as well as the flows in the gas can significantly affect the critical parameters of instability. The influence of a forced gas flow on the stability of thermocapillary convection in a liquid column was investigated theoretically

*andr@icm.krasn.ru
†rii@icm.krasn.ru

by Ryzhkov *et al* [8, 9]. Experimental and numerical study of flows in the liquid bridge with a co–axial gas flow was performed by Gaponenko *et al* [10].

The present work continues the studies of thermocapillary flow control in systems with cylindrical symmetry. We consider an infinite liquid column surrounded by an annular channel of gas, which is bounded externally by the solid wall. The gas is pumped in different directions with respect to the thermocapillary motion of liquid at the interface. It is assumed that the external solid wall can move in vertical direction. The velocity of the wall is determined from the condition of a closed flow in the liquid column. The cases of non–deformable and deformable interface are investigated.

1. Problem Statement

Consider a cylindrical liquid column surrounded by an annular gas channel, which is bounded externally by the solid wall $R = R_g$ (Fig. 1). The interface between liquid and gas is described by the equation $\Gamma = R - R_l - F(t, \varphi, z) = 0$, where the function F characterizes the deviation of the interface from the cylindrical surface of radius R_l. It is assumed that the liquid column and gas channel are infinite in Z direction and the temperature gradient $\partial T/\partial Z = A > 0$ is applied in liquid and gas along Z axis. The gas is pumped with a fixed flow rate Q^G through any cross–section $Z = \text{const}$.

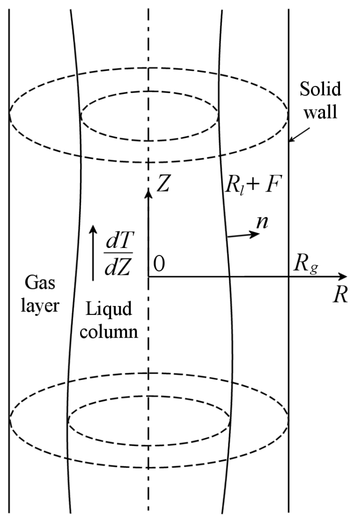

Fig. 1. Geometry of the problem

The flow is described by the velocity vectors $\boldsymbol{U}^{l,g} = (U_r^{l,g}, U_\varphi^{l,g}, U_z^{l,g})$, temperatures $T^{l,g}$, and pressures $P^{l,g}$, where the superscripts l and g are related to liquid and gas, respectively. Liquid and gas phases are characterized by the densities $\rho^{l,g}$, dynamic viscosities $\mu^{l,g}$, thermal conductivities $\kappa^{l,g}$, and thermal diffusivities $\chi^{l,g}$, which are assumed to be constant. The motion of liquid and gas in weightlessness is described by the Navier–Stokes and heat transfer equations (it is supposed that the characteristic velocities are small in comparison with the speed of sound).

Equations for the liquid phase have the form

$$\begin{aligned}
&\frac{d^l U_r^l}{dt} - \frac{(U_\varphi^l)^2}{r} = -\frac{1}{\rho^l}\frac{\partial P^l}{\partial r} + \frac{\mu^l}{\rho^l}\Delta U_r^l - \frac{2}{r^2}\frac{\partial U_\varphi^l}{\partial \varphi} - \frac{U_r^l}{r^2},\\
&\frac{d^l U_\varphi^l}{dt} + \frac{U_r^l U_\varphi^l}{r} = -\frac{1}{\rho^l}\frac{1}{r}\frac{\partial P^l}{\partial \varphi} + \frac{\mu^l}{\rho^l}\Delta U_\varphi^l + \frac{2}{r^2}\frac{\partial U_r^l}{\partial \varphi} - \frac{U_\varphi^l}{r^2},\\
&\frac{d^l U_z^l}{dt} = -\frac{1}{\rho^l}\frac{\partial P^l}{\partial z} + \frac{\mu^l}{\rho^l}\Delta U_z^l,\\
&\frac{\partial U_r^l}{\partial r} + \frac{U_r^l}{r} + \frac{1}{r}\frac{\partial U_\varphi^l}{\partial \varphi} + \frac{\partial U_z^l}{\partial z} = 0,\\
&\frac{d^l T^l}{dt} = \chi^l \Delta T^l,
\end{aligned} \tag{1}$$

where

$$\frac{d^l}{dt} = \frac{\partial}{\partial t} + U_r^l\frac{\partial}{\partial r} + \frac{U_\varphi^l}{r}\frac{\partial}{\partial \varphi} + U_z^l\frac{\partial}{\partial z}, \qquad \Delta = \frac{\partial^2}{\partial r^2} + \frac{1}{r}\frac{\partial}{\partial r} + \frac{1}{r^2}\frac{\partial^2}{\partial \varphi^2} + \frac{\partial^2}{\partial z^2}.$$

The equations for the gas phase have the same form, but the superscript l should be replaced by the superscript g.

The dependence of surface tension on temperature on the interface between two phases is assumed to be linear:

$$\sigma = \sigma_0 - \sigma_T(T - T_0),$$

where T_0 is the solid wall temperature on the circle $Z = 0$.

The continuity of velocities, temperatures, and heat fluxes as well as the kinematic and dynamic conditions must be satisfied on the interface $R = R_l + F(t, \varphi, z)$:

$$\begin{aligned}
&\boldsymbol{U}^l = \boldsymbol{U}^g \equiv \boldsymbol{U},\\
&\frac{\partial \Gamma}{\partial t} + \boldsymbol{U}\cdot\nabla\Gamma = 0,\\
&(\mathcal{P}^l - \mathcal{P}^g)\boldsymbol{n} = 2H\sigma\boldsymbol{n} + \nabla_\Gamma \sigma,\\
&T^l = T^g, \qquad \kappa^l\frac{\partial T^l}{\partial \boldsymbol{n}} = \kappa^g \frac{\partial T^g}{\partial \boldsymbol{n}},
\end{aligned} \tag{2}$$

where $\boldsymbol{U}$ is the velocity vector on the interface, $\mathcal{P}^{l,g} = -p^{l,g}E + 2\mu^{l,g}D(\boldsymbol{U}^{l,g})$ are the stress tensors in liquid and gas phases, $D(\boldsymbol{U}^{l,g})$ are the rate of strain tensors, H is the mean curvature of the interface, ∇_Γ is the surface gradient, and $\boldsymbol{n}$ is the normal unit vector to the interface (Fig. 1).

On the axis $r = 0$, all quantities should be bounded:

$$|\boldsymbol{U}^l|,\ |T^l|,\ |P^l| < \infty \tag{3}$$

On the solid wall of external cylinder $R = R_g$, the following conditions are imposed:

$$\boldsymbol{U}^g = (0,\, 0,\, U_0), \qquad T = AZ + T_0, \tag{4}$$

where U_0 is the constant wall velocity along Z axis. It will be shown below that for unidirectional motion of liquid and gas this velocity is not an independent parameter and can be determined from the other parameters of the problem (provided that the liquid flow rate through any cross–section $Z = \text{const}$ is zero and the gas flow rate is a given constant Q^G).

Let us introduce dimensionless variables according to

$$R = R_l\, r, \qquad Z = R_l\, z, \qquad \boldsymbol{U}^{l,g} = \frac{\mu^l}{\rho^l R_l}\, \boldsymbol{u}^{l,g},$$
$$T^{l,g} - T_0 = AR_l\, \Theta^{l,g}, \qquad P^{l,g} = \rho_{l,g} \left(\frac{\mu^l}{\rho^l R_l}\right)^2 p^{l,g}, \qquad F = R_l f.$$

The time scale is chosen as $\rho^l R_l^2/\mu^l$. The problem is characterized by the following dimensionless parameters:

$$\mathrm{Ma} = \frac{\sigma_T A R_l^2}{\mu^l \chi^l}, \qquad \mathrm{Pr}^l = \frac{\mu^l}{\rho^l \chi^l}, \qquad \mathrm{Ca} = \frac{\sigma_T A R_l}{\sigma_0},$$
$$\rho = \frac{\rho^g}{\rho^l}, \qquad \mu = \frac{\mu^g}{\mu^l}, \qquad \kappa = \frac{\kappa^g}{\kappa^l}, \qquad \chi = \frac{\chi^g}{\chi^l}, \qquad \gamma = \frac{R_g}{R_l},$$

where Ma is the Marangoni number, Pr^l is the liquid Prandtl number, Ca is the capillary number, ρ, μ, κ, χ are the ratios of the corresponding physical properties of gas and liquid, and γ is the ratio of radii. Equations (1) and conditions (2)–(4) are rewritten in dimensionless form.

2. The Basic Stationary Flow

Let us consider a steady axisymmetric flow of liquid and gas in Z direction. The corresponding solution is sought in the form

$$\boldsymbol{u}^{l0} = (0, 0, w^{l0}(r)), \qquad \Theta^{l0} = z + \Theta^{l0}(r), \qquad p^{l0} = Lz + p_0^l, \tag{5}$$
$$\boldsymbol{u}^{g0} = (0, 0, w^{g0}(r)), \qquad \Theta^{g0} = z + \Theta^{g0}(r), \qquad p^{g0} = Gz + p_0^g,$$

where L, G, p_0^l, p_0^g are constants.

It is assumed that the gas–liquid interface is a cylindrical surface of radius $R = R_l$ for the basic stationary flow. On this surface, conditions (2) must be satisfied:

$$w^{l0} = w^{g0}, \tag{6}$$

$$p^{l0} - p^{g0} = \frac{\mathrm{Ma}}{\mathrm{Pr}^l} \left(\frac{1}{\mathrm{Ca}} - \Theta^{l0}\right), \qquad \frac{\partial w^{l0}}{\partial r} - \mu \frac{\partial w^{g0}}{\partial r} = -\frac{\mathrm{Ma}}{\mathrm{Pr}^l} \frac{\partial \Theta^{l0}}{\partial z}, \tag{7}$$

$$\Theta^{l0} = \Theta^{g0}, \qquad \frac{\partial \Theta^{l0}}{\partial r} = \kappa \frac{\partial \Theta^{g0}}{\partial r}. \tag{8}$$

On the solid wall $r = \gamma$, the value of wall vertical velocity and linear temperature distribution are imposed:

$$w^{g0} = w_0, \qquad \Theta^{g0} = z, \tag{9}$$

where $w_0 = \rho_l R_l \mu_l^{-1} U_0$. We require that the liquid flow rate through any crossection $z = \mathrm{const}$ is zero:

$$\int_0^1 r\, w^{l0}(r)\, dr = 0. \tag{10}$$

This condition is satisfied in a physical liquid bridge, which is bounded by two rods in axial direction [2]. Further, we specify a constant gas flow rate through any crossection $z = \mathrm{const}$:

$$Q^g = 2\pi \int_1^\gamma r\, w^{g0}(r)\, dr, \tag{11}$$

where $Q^g = \rho_l (\mu^l R_l)^{-1} Q^G$. For convenient presentation of results, we will use the quantity $Q = 10^{-3}\, Q^g$ instead of Q^g below.

Substituting representation (5) into equations of motion and satisfying conditions (3), (6)–(11), we obtain the solution

$$
\begin{aligned}
&w^{l0} = \Big(G - \frac{\mathrm{Ma}}{\mathrm{Pr}^l}\Big)\Big(\frac{r^2}{4} - \frac{1}{8}\Big), \qquad w^{g0} = \frac{G}{4\mu}\Big(r^2 - 1 + \frac{\mu}{2}\Big) + \frac{\mathrm{Ma}}{2\mu \mathrm{Pr}^l}\Big(\ln r - \frac{\mu}{4}\Big),\\
&p^{l0} = \Big(G - \frac{\mathrm{Ma}}{\mathrm{Pr}^l}\Big) z + p_0^g + \frac{\mathrm{Ma}}{\mathrm{Ca}\,\mathrm{Pr}^l} + \frac{\mathrm{Ma}}{64\chi}\Big(G\Big(\frac{3}{\mu} - 2\Big) + \frac{2\mathrm{Ma}}{\mathrm{Pr}^l}\Big(\frac{4}{\mu} + 1\Big)\Big) - \frac{\mathrm{Ma}}{\mathrm{Pr}^l} A_2,\\
&p^{g0} = Gz + p_0^g, \qquad\qquad (12)\\
&\Theta^{l0} = \frac{\mathrm{Pr}^l G - \mathrm{Ma}}{64}\big(r^4 - 2r^2\big) + A_3 + z,\\
&\Theta^{g0} = \frac{r^2}{64\mu\chi}\Big(\mathrm{Pr}^l G\big(r^2 + 2(\mu - 2)\big) + 2\mathrm{Ma}(4\ln r - 4 - \mu)\Big) + A_1 \ln r + A_2 + z,
\end{aligned}
$$

where

$$
\begin{aligned}
A_1 &= \frac{1}{16\chi}\Big[\mathrm{Pr}^l G\Big(\frac{1}{\mu} - 1\Big) + \mathrm{Ma}\Big(\frac{2}{\mu} + 1\Big)\Big],\\
A_2 &= \frac{1}{64\chi}\Big[\mathrm{Pr}^l G\Big(\ln\gamma\Big(4 - \frac{4}{\mu}\Big) + 2\gamma^2\Big(\frac{2}{\mu} - 1\Big) - \frac{\gamma^4}{\mu}\Big) - 2\mathrm{Ma}\Big(2\ln\gamma\Big(\frac{2\gamma^2 + 2}{\mu} + 1\Big) - \gamma^2\Big(\frac{4}{\mu} + 1\Big)\Big)\Big],\\
A_3 &= \frac{1}{64}\Big[\mathrm{Pr}^l G\Big(1 + \frac{2}{\chi} - \frac{3}{\mu\chi}\Big) - \mathrm{Ma}\Big(1 + \frac{2}{\chi} + \frac{8}{\mu\chi}\Big)\Big] + A_2.
\end{aligned}
$$

The constant p_0^g in solution (12) specifies the gas pressure on the plane $z = 0$. The dimensionless gas pressure gradient is related to the gas flow rate Q by the formula

$$
G = \frac{8\mu\,\pi^{-1}10^3 Q + \mathrm{Ma}\,(\mathrm{Pr}^l)^{-1}((\gamma^2 - 1)(\mu + 2) - 4\gamma^2\ln\gamma)}{\gamma^2(\gamma^2 + \mu - 2) - \mu + 1}.
$$

It should be noted that the solid wall velocity in Z direction (see condition (4)) is determined by the value of function w^{g0} at $r = \gamma$.

In this paper, we investigate a two–phase system of silicon oil (2 cSt) – Air in cylindrical layers with aspect ratio $\gamma = 2$. The corresponding physical properties and dimensionless parameters are given in Table 1.

Table 1.

σ_0, 10^{-3} N/m 19.50	σ_T, 10^{-5} N/mK 6.40	ρ^l, kg/m^3 860	μ^l, 10^{-3} Pa·s 1.72	κ^l, W/mK 0.10	χ^l, 10^{-8} m^2/s 6.80
ρ 0.00136	μ 0.01087	κ 0.26139	χ 331.32	Pr^l 29.41	

The velocity and temperature profiles in the cross–section $z = \mathrm{const}$ are shown in Fig. 2 for different gas flow rates. When there is no gas pumping (curve 2), the liquid on the interface is moving against the temperature gradient and entrains the gas in the same direction. As the gas velocity is much higher than the liquid velocity, the corresponding profiles are shown in Figs. 2a and 2b with different scales.

The variation of temperature in radial direction is caused by the motion of liquid from hot to cold region near the interface and in the opposite direction near the axis $r = 0$. When $Q > 0$, the direction of gas pumping is opposite to the thermocapillary motion on the interface. It results

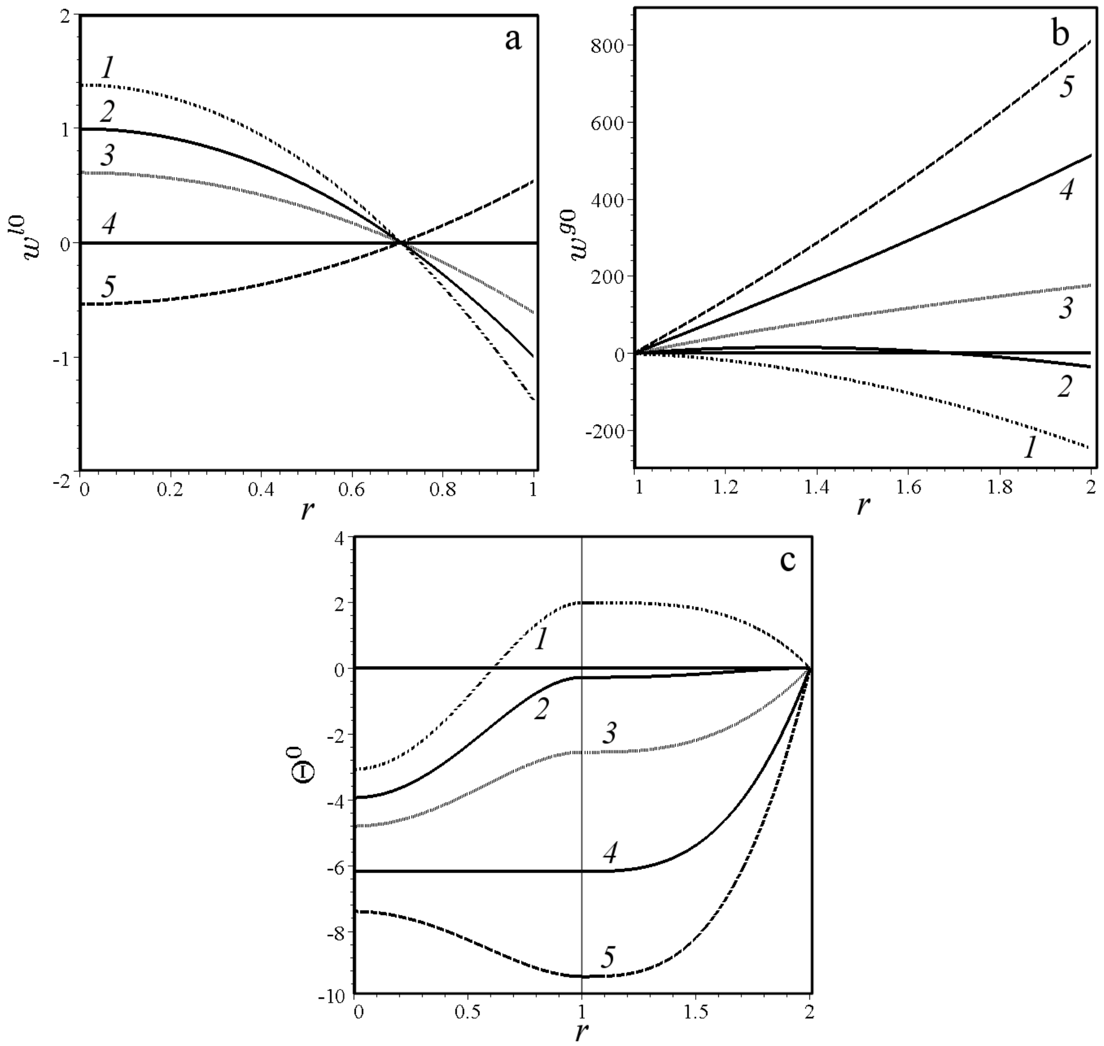

Fig. 2. The velocity profiles in liquid (a) and gas (b) phases and temperature profiles (c) for gas flow rates $Q = -1$ (curve 1), $Q = 0$ (curve 2), $Q = 1$ (curve 3), $Q = 2.6$ (curve 4), $Q = 4$ (curve 5). The Marangoni number is $\mathrm{Ma} = 150$

in the decrease of liquid velocity (curve 3). This effect becomes stronger with increasing Q. At some critical value $Q = Q_0$, the velocity of liquid on the interface (as well as inside the liquid column) vanishes (curve 4). The corresponding value of gas flow rate depends linearly on the Marangoni number Ma:

$$Q_0 = 10^{-3}\frac{\mathrm{Ma}}{\mathrm{Pr}^l}\,\frac{\pi}{8\mu}\,(\gamma^4 + 4\gamma^2(\ln\gamma - 1) + 3). \tag{13}$$

With the further increase of gas flow rate $(Q > Q_0)$ one observes the inversion of velocity profile in liquid. The liquid on the interface moves in the direction of gas pumping (curve 5). For negative values of gas flow rate $(Q < 0)$, the direction of gas pumping coincides with the thermocapillary motion on the interface and the liquid velocity increases (curve 1).

It should be noted that solution (12) was previously obtained in [11] in dimensional form. Analogue of solution (12) for two plane layers of immiscible liquids was found in [12]. Convective flows caused by thermocapillary effect and longitudinal pressure gradient in two–layer systems formed by two binary mixtures or a binary mixture and a viscous fluid were investigated in [13,14].

3. Stability Problem

In this section, we proceed to the linear stability analysis of the basic stationary flow (12) with respect to small perturbations. The velocity, temperature, and pressure fields are represented as a sum of the basic state and small perturbations

$$\boldsymbol{u}^{l,g} = \boldsymbol{u}^{l0,\,g0} + \widetilde{\boldsymbol{u}}^{l,g}, \qquad p^{l,g} = p^{l0,\,g0} + \widetilde{p}^{l,g}, \qquad \Theta^{l,g} = \Theta^{l0,\,g0} + \widetilde{\Theta}^{l,g}.$$

The perturbed interface is described by the equation $r = 1 + \widetilde{f}(r, \varphi, z)$. Let us substitute these expressions into the equations of motion and boundary conditions and linearize them around the basic state. The perturbations are sought in the normal form

$$\big(\widetilde{\boldsymbol{u}}^{l,g}, \widetilde{p}^{l,g}, \widetilde{\Theta}^{l,g}, \widetilde{f}\big) = \big(u_{l,g}(r),\, v_{l,g}(r),\, w_{l,g}(r),\, p_{l,g}(r),\, \theta_{l,g}(r),\, \xi\big)\, \exp\big(-\lambda t + i(kz + m\varphi)\big),$$

where $\lambda = \lambda_r + i\omega$ is the complex growth rate, k and m are the wave numbers in z and φ directions, respectively, and ξ is a constant. The equations for amplitudes of perturbations in the liquid have the form

$$\begin{aligned}
&\left(D - k^2 - \frac{m^2+1}{r^2} + \lambda - ik\, w^{l0}\right) u_l - \frac{2im}{r^2}\, v_l - p_l' = 0,\\
&\left(D - k^2 - \frac{m^2+1}{r^2} + \lambda - ik\, w^{l0}\right) v_l + \frac{2im}{r^2}\, u_l - \frac{im}{r} p_l = 0,\\
&\left(D - k^2 - \frac{m^2}{r^2} + \lambda - ik\, w^{l0}\right) w_l - (w^{l0})' u_l - ikp_l = 0, \qquad (14)\\
&\left(D - k^2 - \frac{m^2}{r^2} + \mathrm{Pr}^l\big(\lambda - ik\, w^{l0}\big)\right) \theta_l - \mathrm{Pr}^l\big(w_l + (\Theta^{l0})' u_l\big) = 0,\\
&u_l' + \frac{u_l}{r} + \frac{im}{r} v_l + ik\, w_l = 0.
\end{aligned}$$

The corresponding equations for the gas phase are written as

$$\begin{aligned}
&\left(D - k^2 - \frac{m^2+1}{r^2} + \frac{\rho}{\mu}\big(\lambda - ik\, w^{g0}\big)\right) u_g - \frac{2im}{r^2}\, v_g - \frac{p_g'}{\mu} = 0,\\
&\left(D - k^2 - \frac{m^2+1}{r^2} + \frac{\rho}{\mu}\big(\lambda - ik\, w^{g0}\big)\right) v_g + \frac{2im}{r^2}\, u_g - \frac{im}{\mu r} p_g = 0,\\
&\left(D - k^2 - \frac{m^2}{r^2} + \frac{\rho}{\mu}\big(\lambda - ik\, w^{g0}\big)\right) w_g - \frac{\rho}{\mu}(w^{g0})' u_g - \frac{ik}{\mu} p_g = 0, \qquad (15)
\end{aligned}$$

$$\begin{aligned}
&\left(D - k^2 - \frac{m^2}{r^2} + \frac{\mathrm{Pr}^l}{\chi}\big(\lambda - ik\, w^{g0}\big)\right) \theta_g - \frac{\mathrm{Pr}^l}{\chi}\big(w_g + (\Theta^{g0})' u_g\big) = 0,\\
&u_g' + \frac{u_g}{r} + \frac{im}{r} v_g + ik\, w_g = 0.
\end{aligned}$$

Here $D = d^2/dr^2 + r^{-1}d/dr$ and the prime corresponds to the derivative d/dr. The amplitudes of perturbations satisfy the following boundary conditions:

$$r = \gamma: \qquad u_g = v_g = w_g = \theta_g = 0; \tag{16}$$

$$r = 1: \qquad u_l - u_g = 0, \qquad v_l - v_g = 0, \qquad w_l + (w^{l0})'\xi - w_g - (w^{g0})'\xi = 0, \tag{17}$$

$$u_l + (\lambda - ik\,(w^{l0})')\,\xi = 0, \tag{18}$$

$$p_g - p_l + 2\big(u_l' - ik(w^{l0})'\xi\big) - 2\mu\big(u_g' - ik(w^{g0})'\xi\big) -$$

$$-\frac{\mathrm{Ma}}{\mathrm{Pr}^l}\,\theta_l + \frac{\mathrm{Ma}}{\mathrm{Pr}^l}\left(\frac{1}{\mathrm{Ca}} - \Theta^{l0}\right)(m^2 + k^2 - 1)\,\xi = 0, \tag{19}$$

$$im\,u_l + v_l' - v_l - \mu\big(im\,u_g + v_g' - v_g\big) + \frac{\mathrm{Ma}}{\mathrm{Pr}^l}\,im\,\theta_l = 0, \tag{20}$$

$$ik\,u_l + (w^{l0})''\xi + w_l' - \mu\big(ik\,u_g + (w^{g0})''\xi + w_g'\big) + \frac{\mathrm{Ma}}{\mathrm{Pr}^l}\,ik\,\theta_l = 0, \tag{21}$$

$$\theta_l' + ((\Theta^{l0})'' - ik)\,\xi - \kappa\big(\theta_g' + ((\Theta^{g0})'' - ik)\,\xi\big) = 0, \tag{22}$$

$$\theta_l - \theta_g = 0, \tag{23}$$

$$r = 0: \qquad |u_l|,\ |v_l|,\ |w_l|,\ |\theta_l|,\ |p_l|\ < \infty. \tag{24}$$

The amplitude of interface perturbation is found from condition (21) taking into account (12):

$$\xi = \left(\frac{(\mathrm{Pr}^l G - \mathrm{Ma})(\chi - \kappa)}{8\chi} + ik(\kappa - 1)\right)^{-1}(\kappa\theta_g' - \theta_l')\Big|_{r=1}.$$

To specify the values of unknown functions near $r = 0$, the asymptotic expansions are used (the corresponding formulas can be found in [9]).

It should be noted that the last term in boundary condition (19) contains the factor $\mathrm{Ca}^{-1} - \Theta^{l0}(r) - z$, see solution (12). The dependence of boundary condition on z does not allow us to seek a solution periodic in z. But this dependence can be ignored provided that the dimensionless wavelength of perturbation is much smaller than Ca^{-1} [1]. In terms of wave number, it is equivalent to $k \gg 2\pi\mathrm{Ca}$. This inequality can be rewritten in the form

$$k > 2\pi\frac{10\,\mathrm{Ma}}{\mathrm{Pr}^l\mathrm{W}}, \tag{25}$$

where $\mathrm{W} = \sigma_0\rho^l R_l(\mu^l)^{-2}$ ($\mathrm{W} = 5669$ for the system considered here). The factor 10 was introduced into the right–hand side of (25) for concreteness.

Problem (14)–(24) is invariant under the change of variables

$$m \to -m, \qquad v_{l,g} \to -v_{l,g}. \tag{26}$$

So, one can assume that $m \geqslant 0$ since the consideration of negative m does not lead to the extension of the spectrum. It should also be noted that due to continuity in φ, the spectrum of m values is discrete ($m = 0, 1, 2, \dots$). The considered problem is also invariant under the change

$$k \to -k, \qquad \lambda \to \overline{\lambda},$$

$$u_{l,g} \to \overline{u}_{l,g}, \quad v_{l,g} \to -\overline{v}_{l,g}, \quad w_{l,g} \to \overline{w}_{l,g}, \quad p_{l,g} \to \overline{p}_{l,g}, \quad \theta_{l,g} \to \overline{\theta}_{l,g}, \tag{27}$$

where the complex conjugate is denoted by the bar.

Consider two solutions obtained by applying transformations (26) and (27) to an arbitrary solution of the given problem. It can be easily seen that one of these solutions is the complex conjugate of the other. As physical perturbations are obtained by taking real parts of complex eigenfunctions, transformations (26) and (27) produce the same physical solutions. The only exception here is the case $m = 0$, in which $v_{l,g} = 0$ and transformation (26) reduces to an identical one.

It follows from (27) that the oscillatory instability develops in the form of two waves with opposite wave numbers k and angular frequencies ω. These waves propagate in directions given by the angles $\pm\,\mathrm{arctg}(m/|k|)$ with respect to the positive direction of z axis.

To solve problem (14)–(24), we employ the Runge–Kutta–Merson method of 5th order with orthogonalization in combination with the shooting procedure. The details on the application of this method to a similar problem can be found in [8, 9]. For the given values of parameters, the left–hand side of the following dispersion relation is calculated:

$$\Pi\big(\lambda, m, k, \mathrm{Ma}, \mathrm{Pr}^l, \rho, \mu, \kappa, \chi, \gamma, Q\big) = 0.$$

This relation determines the spectrum of complex growth rates λ. It allows one to find the stability boundaries in the parameter space.

4. Results for Non–deformable Interface

If the surface tension σ_0 is large, then the interface can be considered as non–deformable. In this case, the capillary number Ca is small. Multiplying boundary condition (19) by Ca and taking the limit as $\mathrm{Ca} \to 0$, we find $\xi = 0$, i.e. the interface perturbation vanishes. Boundary conditions (17)–(23) become

$$\begin{aligned} r = 1: \quad & u_l = u_g = 0, \qquad v_l = v_g, \qquad w_l = w_g, \\ & v_l' - v_l - \mu(v_g' - v_g) + \frac{\mathrm{Ma}}{\mathrm{Pr}^l}\, im\,\theta_l = 0, \qquad w_l' - \mu w_g' + \frac{\mathrm{Ma}}{\mathrm{Pr}^l}\, ik\,\theta_l = 0, \\ & \theta_l = \theta_g, \qquad \theta_l' = \kappa\,\theta_g'. \end{aligned}$$

Typical structure of neutral curves on the plane (k, Ma) is shown in Fig. 3a for the gas flow rate $Q = 2$. These curves correspond to oscillatory instability. The dependence of dimensionless critical frequency ω on the wave number k is presented in Fig. 3b, c (different scales on Ma axis are used for different curves).

Let us first consider the case $\mathrm{Ma} > \mathrm{Ma}(Q_0)$, where the latter value of the Marangoni number is determined from condition (13) with $Q_0 = 2$ (when $\mathrm{Ma} = \mathrm{Ma}(Q_0)$, the motion of liquid vanishes, see also Fig. 4a below). In the above range of Ma values, the direction of gas pumping is opposite to the thermocapillary motion on the interface. The increase of gas flow rate decreases the liquid velocity on the interface (Fig. 2a). In this case, the critical instability mode is $m = 1$ (curve 1C in Fig. 3a). One can see that there is a change of the most unstable eigenmode at $k = 1.6$ to that with a different frequency (the sign and absolute value of the frequency change, see Fig. 3c). The neutral curve for the mode $m = 2$ has a similar structure.

Now we proceed to the case $0 < \mathrm{Ma} < \mathrm{Ma}(Q_0)$, where the inversion of velocity profile in the liquid is observed (see Fig. 2a). The mode $m = 1$ is critical here as well. The system is unstable in a closed domain, which is bounded by the curves 1A, 1B and the line $k = 0$. The minimum of curve 1A and maximum of curve 1B correspond to $k = \omega = 0$. So, the instability is associated with the growth of long–wave disturbances. If cylindrical layers are bounded in the z direction (which is always the case in the experiment), then this type of instability sets in at the largest

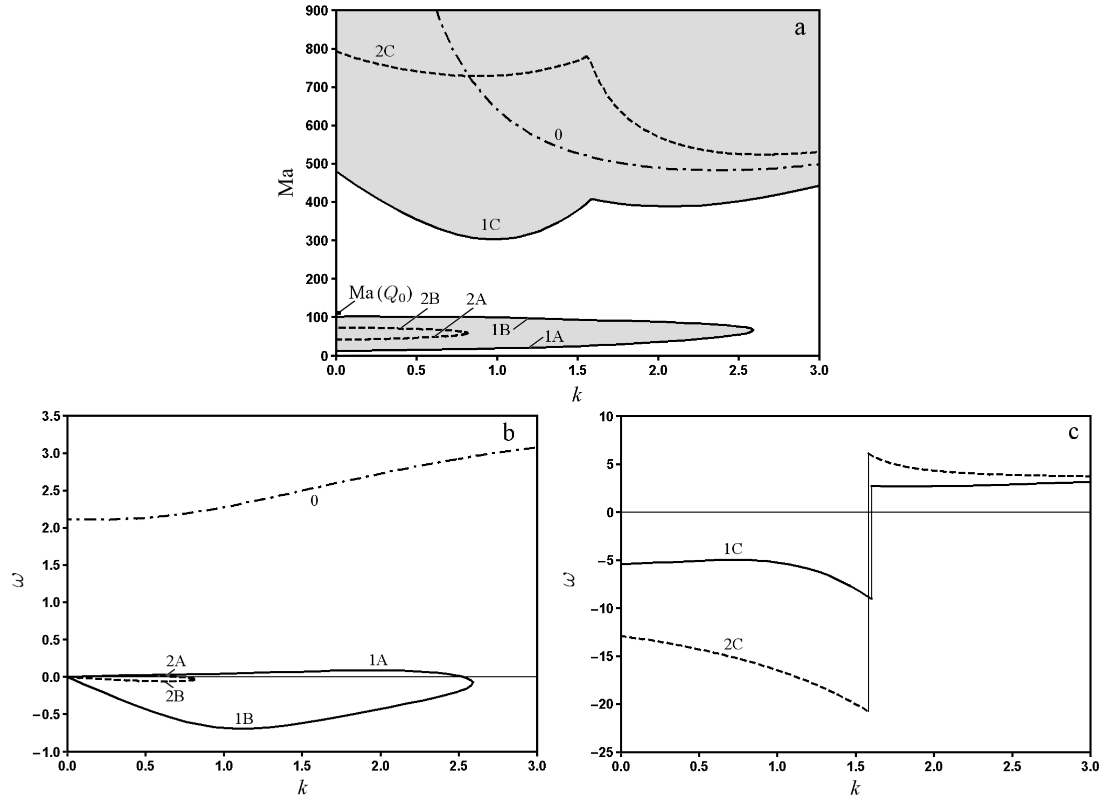

Fig. 3. Neutral curves for gas flow rate $Q = 2$: critical Marangoni number (a) and critical frequency (b, c). The modes $m = 0$ (0), $m = 1$ (1A, 1B, 1C) and $m = 2$ (2A, 2B, 2C) are shown. The system is unstable in the shaded area

possible wavelength (which is equal to the vertical dimension of the system). The instability region for the mode $m = 2$ has a similar structure and lies inside the region for the mode $m = 1$.

The dependence of critical parameters of instability on the gas flow rate Q is shown in Fig. 4. The critical mode is always $m = 1$. In the absence of gas pumping ($Q = 0$), the system becomes unstable when the Marangoni number exceeds the critical value of $\mathrm{Ma} = 288,11$. If the direction of pumping coincides with thermocapillary motion on the interface ($Q < 0$), then the velocity of stationary flow on the interface increases with increasing the absolute value of gas flow rate. In this case, the system becomes unstable at smaller Ma (see curve E for $Q < 0$). When the gas flow rate is changing in negative direction, the absolute values of critical wave number and frequency are decreasing. In the region $0 < Q < Q_0(\mathrm{Ma})$, the direction of gas pumping is opposite to the thermocapillary motion on the interface and the velocity of stationary flow decreases with increasing Q. As a result, the instability threshold slightly increases. The increase of gas flow rate leads to the change of critical mode at $Q = 0,2$ (curve D). The absolute value of wave number k decreases sharply, while the corresponding value of critical frequency increases (in magnitude). The growth of critical Marangoni number is slowed down with the further increase of Q. The Marangoni number reaches the maximum value and then starts to decrease until $Q = 3,63$, $\mathrm{Ma} = 247$. For larger values of gas flow rate in the range $0 < Q < Q_0(\mathrm{Ma})$, the system is always unstable. Note that in the above range, there is an additional instability region close to the line $Q = Q_0(\mathrm{Ma})$. This region is bounded from above by curve C. At the line $Q = Q_0(\mathrm{Ma})$, the velocity in the liquid phase vanishes. This regime is stable for $\mathrm{Ma} < 192,8$ and $Q_0 < 3,3$.

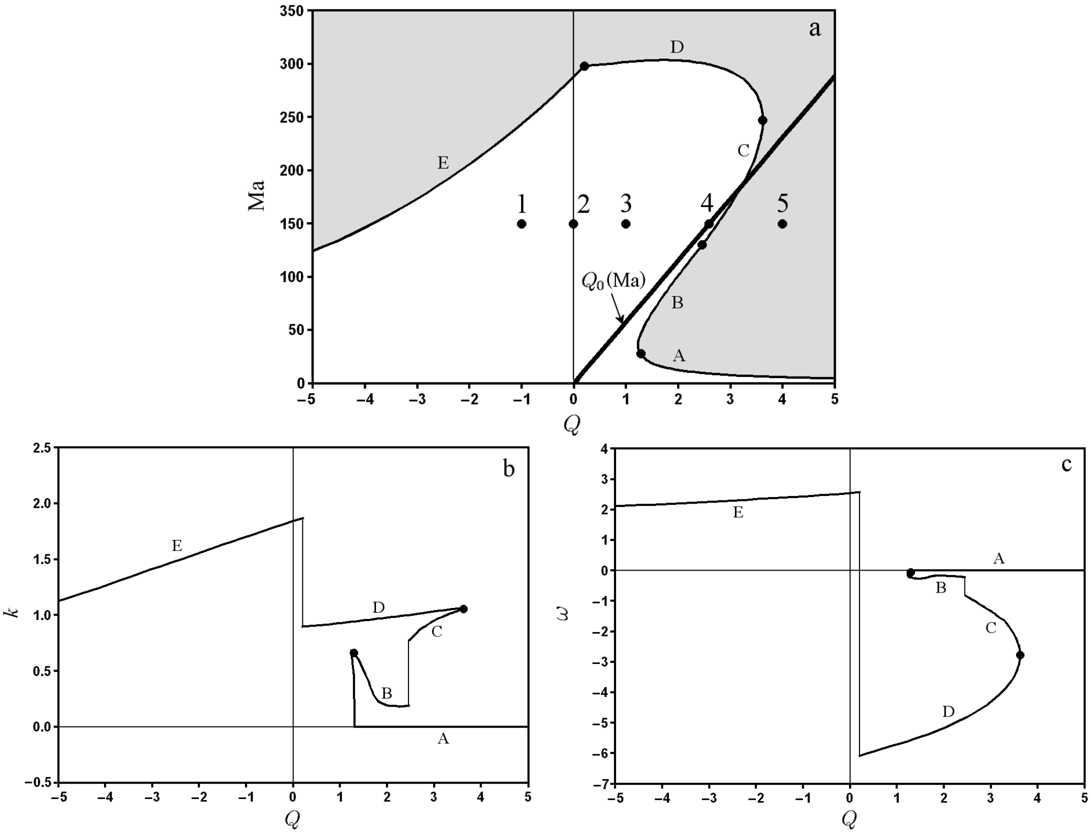

Fig. 4. The dependence of critical parameters of instability on the gas flow rate Q: Marangoni number (a), wave number (b), and angular frequency (c); the critical mode is $m = 1$. Points 1–5 on the plane (Q, Ma) correspond to profiles 1–5 in Fig. 2. The system is unstable in the shaded areas

In the case $Q > Q_0(\mathrm{Ma})$, large gas flow rate causes the inversion of velocity profile in the liquid (the direction of liquid flow on the interface coincides with the direction of gas pumping), see Fig. 2a. Here the instability region is bounded by curves A and B. Curve A corresponds to long–wave disturbances ($k = \omega = 0$), but in the vicinity of its connection with curve B (at the point $Q = 1,23$, $\mathrm{Ma} = 36$), the critical wave number becomes non–zero. The transition from curve B to curve C at the point $Q = 2,46$, $\mathrm{Ma} = 130,2$ is characterized by the change of instability mode (critical wave number and critical frequency show an abrupt increase in magnitude).

5. Results for Deformable Interface

Let us proceed to the case of deformable interface. In this case, there is a limitation on the values of wave number k given by inequality (25). In what follows, we will present neutral curves in a wide range of wave numbers including the region near $k = 0$. However, the only physically meaningful results are those that satisfy condition (25).

The neutral curves for axisymmetric perturbations ($m = 0$) in the absence of gas pumping ($Q = 0$) are shown in Fig. 5. One can see that there are three modes associated with different instability mechanisms [1]. Curve 1 corresponds to the thermal mode, which is a wave travelling fast in positive direction of z axis (opposite to the basic flow on the interface). Thermal mode is

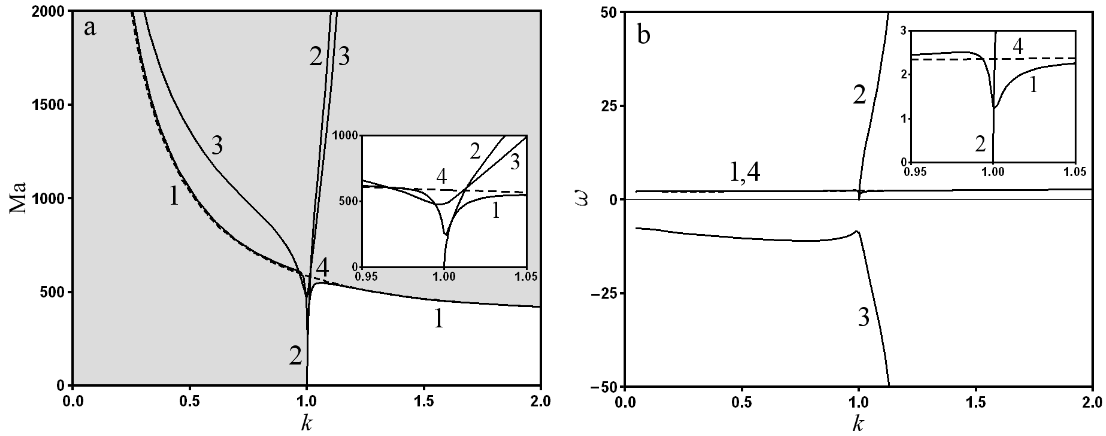

Fig. 5. Neutral curves for $Q = 0$, $m = 0$: critical Marangoni number (a) and critical frequency (b). 1 — thermal mode, 2 — capillary mode, 3 — hydrodynamic mode, 4 — neutral curve for non–deformable interface. The behavior of neutral curves near $k = 1$ is shown on the inset. The system is unstable in the shaded area

caused by thermal non-homogeneity in liquid and gas and associated thermocapillary effect. This instability mechanism exists in the case of non–deformable interface as well. The corresponding curve 4 coincides with curve 1 almost everywhere (except the neighborhood of $k = 1$). Curve 2 characterizes the capillary mode, which is related to the Rayleigh instability (the height of a liquid cylinder of radius R cannot be greater than $2\pi R$). The capillary mode is monotonic for Ma $= 0$, but it becomes oscillatory for Ma > 0. The capillary wave is travelling slowly in the opposite direction to the basic flow on the interface. The propagation speed increases with increasing the Marangoni number. Curve 3 corresponds to hydrodynamic mode, which is a wave travelling fast in negative direction of z axis (along the basic flow on the interface). It is related to the hydrodynamic instability in liquid and gas.

Let us investigate the influence of gas pumping on the behavior of different instability modes for axisymmetric perturbations ($m = 0$). The neutral curves for thermal mode are shown in Fig. 6 for different values of dimensionless gas flow rate. When $Q > 0$, the direction of pumping is opposite to the thermocapillary flow on the interface. The increase of gas flow rate has a stabilizing effect on the thermal mode (see also Fig. 4). In contrast to the case of non–deformable interface, the neutral curve has a sharp minimum near $k = 1$. Calculations show that the opposite direction of gas pumping ($Q < 0$) has a destabilizing effect on the thermal mode.

The neutral curves for capillary mode are shown in Fig. 7. It was already noted that the capillary mode is monotonic when Ma $= 0$ and $Q = 0$. In the presence of gas pumping ($Q > 0$), the capillary mode becomes oscillatory even for Ma $= 0$, see Fig. 7b. The instability region slightly extends to larger wave numbers. However, for large values of Ma, there is a slight narrowing of the instability region.

The neutral curves for hydrodynamic mode are shown in Fig. 8. When gas is pumped in the opposite direction to the basic flow on the interface ($Q > 0$), the velocity of liquid decreases, and hydrodynamic mode becomes more stable. Calculations show that the opposite direction of gas pumping ($Q < 0$) has a destabilizing effect on this mode.

The neutral curves for non–axisymmetric perturbations ($m = 1$) are shown in Fig. 9. Curves 1 and 2 are thermal modes associated with thermocapillary instability of the basic flow. They correspond to spiral waves travelling fast in positive (curve 1) and negative (curve 2) directions of z axis (along and opposite to the basic flow, respectively). Note that according to (27), the spiral

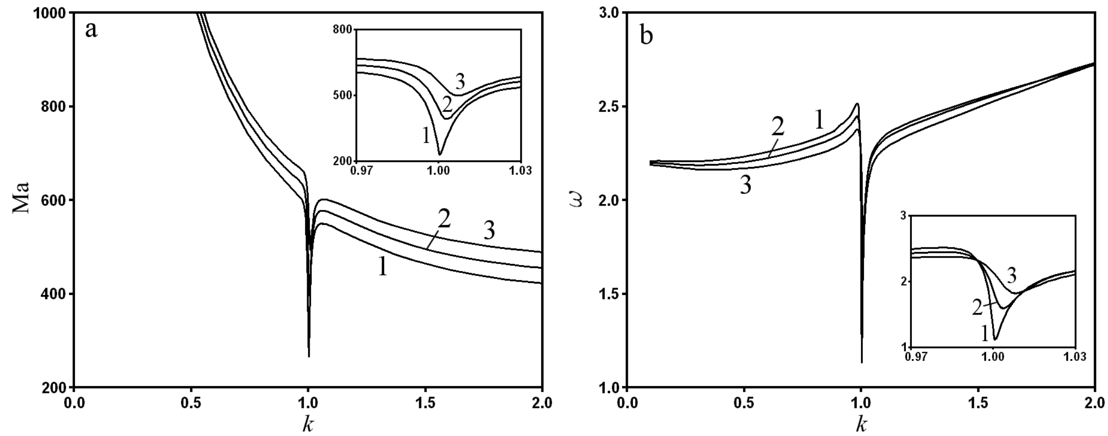

Fig. 6. The dependence of thermal mode $m = 0$ on the dimensionless gas flow rate: critical Marangoni number (a) and critical frequency (b). $1 - Q = 0$, $2 - Q = 1$, $3 - Q = 2$

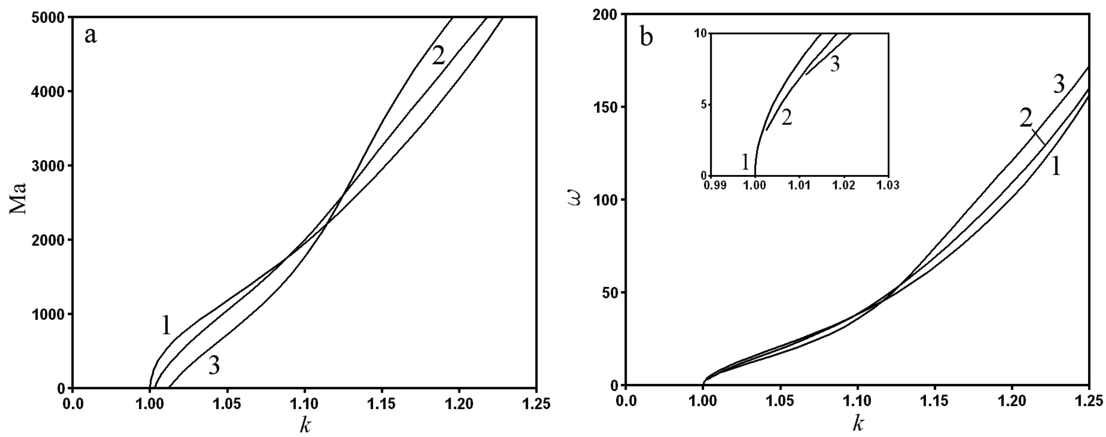

Fig. 7. The dependence of capillary mode $m = 0$ on the dimensionless gas flow rate: critical Marangoni number (a) and critical frequency (b). $1 - Q = 0$, $2 - Q = 1$, $3 - Q = 2$

waves appear in pairs and propagate in the directions given by the angles $\pm\,\mathrm{arctg}(m/|k|)$ with respect to positive or negative direction of z axis. This instability mechanism exists in the case of non–deformable interface as well. The corresponding curves 1a and 2a coincide with curves 1 and 2 almost everywhere (except the neighborhood of $k = 0$). However, in this neighborhood condition (25) is violated (the area of admissible wave numbers is bounded from the left by line 4 in Fig. 9a). Note that in the case of deformable interface there appears a new mode in the region of small wave numbers (curve 3). Calculations shown that gas pumping along (opposite to) the basic flow on the interface destabilizes (stabilizes) the mode $m = 1$.

Conclusion

In this work, we have investigated thermocapillary flows and their stability in an infinite liquid column surrounded by an annular channel of gas. The latter is bounded by the cylindrical solid wall, which can move in vertical direction. Possible stationary flow regimes and their stability are investigated. The comparison between results for non–deformable and deformable interface is performed.

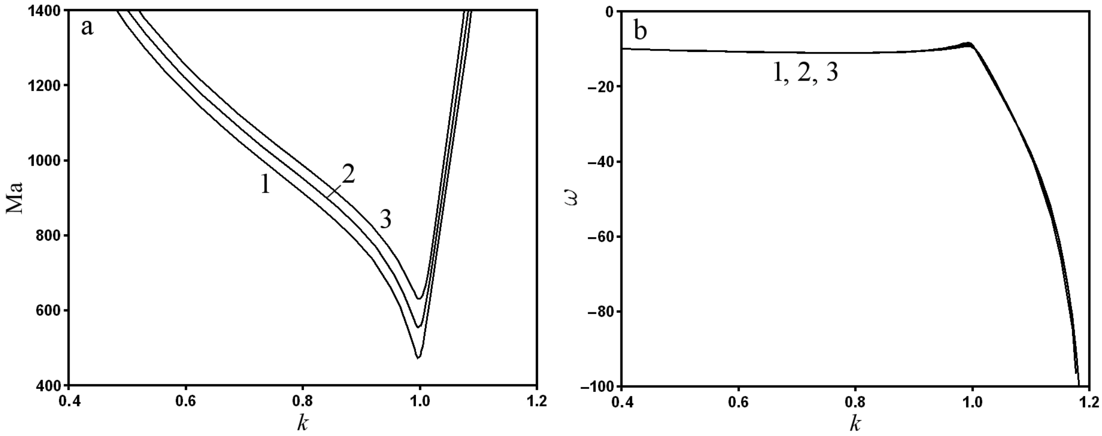

Fig. 8. The dependence of hydrodynamic mode $m = 0$ on the dimensionless gas flow rate: critical Marangoni number (a) and critical frequency (b). 1 — $Q = 0$, 2 — $Q = 1$, 3 — $Q = 2$

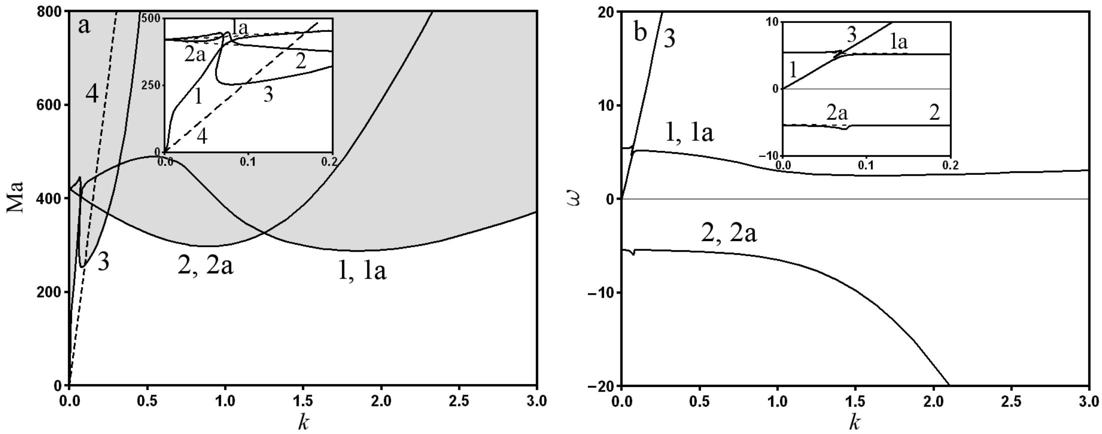

Fig. 9. Neutral curve for $Q = 0$, $m = 1$: critical Marangoni number (a) and critical frequency (b). 1,2,3 — modes for deformable interface, 1a, 2a — modes for non–deformable interface, 4 — line, which bounds the values of wave number k according to (25). The behavior of neutral curves near $k = 0$ is shown on the inset. The system is unstable in the shaded area

This work is supported by the RFBR (project 11-01-00283-a) and Interdisciplinary Project of Fundamental Research no. 38.

References

[1] V.K.Andreev, V.E.Zakhvataev, E.A.Raybitskii, Thermocapillary instability, Novosibirsk, Nauka, 2000 (in Russian).

[2] H.C.Kuhlmann, Thermocapillary Convection in models of crystal growth, Berlin, Springer, 1999.

[3] B.Feuerbacher, H.W.Hamacher, R.J.Naumann, Materials Science in Space, Springer Verlag, Berlin, 1986.

[4] J-J.Xu, S.H.Davis, Convective thermocapillary instabilities in liquid bridges, *Physics of Fluids*, **5**(1984), no. 1, 1102–1107.

[5] I.I.Ryzhkov, Thermocapillary instabilities in liquid bridges revisited, *Physics of Fluids*, **23**(2011), no. 8, 082103.

[6] D.Schwabe, Hydrothermal waves in a liquid bridge with aspect ratio near the Rayleigh limit under microgravity, *Physics of Fluids*, **17**(2005), no. 11, 112104.

[7] M.Irikura, Y.Arakawa, I.Ueno, H.Kawamura, Effect of ambient fluid flow upon onset of oscillatory thermocapillary convection in half–zone liquid bridges, *Microgravity Science and Technology*, **16**(2005), no. 1, 176–180.

[8] I.I.Ryzhkov, Thermocapillary convection stability in a cylindrically symmetric two–phase system, *Fluid Dynamics*, **45**(2010), no. 6, 866–879.

[9] I.I.Ryzhkov, V.Shevtsova, Thermocapillary instabilities in liquid columns under co- and counter-current gas flow, *International Journal of Heat and Mass Transfer*, **55**(2012), no. 4, 1236-1245.

[10] Y.Gaponenko, A.Mialdun, V.Shevtsova, Shear driven two-phase flows in vertical cylindrical duct, *International Journal of Multiphase Flow*, **39**(2011), 205–215.

[11] V.K.Andreev, V.B.Bekezhanova, Stability of non–isothermal flows, Krasnoyarsk, Siberian Federal University, 2010 (in Russian).

[12] L.G.Napolitano, Plane Marangoni-Poiseuille flow of two immiscible fluids, *Acta Astronautica*, **7**(1980), no. 4–5, 461–478.

[13] V.K.Andreev, On properties of solution of a boundary value problem describing simultaneous flow of two binary mixtures. *Proceed. of the Steklov Inst. of Math.* **261**(2008), Suppl. 1, S1–S14.

[14] V.K.Andreev, Evolution of the joint motion of two viscous heat–conducting fluids in a plane layer under the action of an unsteady pressure gradient, *Journal of Applied Mechanics and Technical Physics*, **49**(2008), no. 4, 598–609.

О термокапиллярной неустойчивости жидкого цилиндра, обдуваемого потоком газа

Виктор К. Андреев
Илья И. Рыжков

Проведено исследование термокапиллярных течений и их устойчивости в бесконечном жидком цилиндре, окруженном коаксиальным слоем газа с заданным расходом. Слой газа ограничен твердой цилиндрической поверхностью, которая может перемещаться в вертикальном направлении. В слоях задан постоянный осевой градиент температуры. Найдено точное решение уравнений движения, описывающее стационарное течение в данной двухфазной системе. Изучены возможные режимы течений и их устойчивость в линейном приближении. Рассмотрены случаи недеформируемой и деформируемой границы раздела.

Ключевые слова: термокапиллярная неустойчивость, двухфазная система, жидкий цилиндр.